Cu Heavy Wirebonding for High Power Device Interconnection

Baik-Woo Lee, Chang-Sik Kim, Changmo Jeong, Younghun Byun, Jeong-Won Yoon,
Che-Heung Kim, Seong Woon Booh, U-in Chung
Samsung Advanced Institute of Technology, Samsung Electronics
Yongin, Kyeong-gi Province, 446712 South Korea
Tel: +82-31-280-8426
Email: baikwoo.lee@samsung.com

Abstract

To replace conventional Al heavy wire bonding in interconnecting power devices, we have explored the use of Cu heavy wire bonding, which offers superior electrical, mechanical, and thermal properties compared to Al wires that leads to better interconnection reliability. Chip pad metallizations that are strong enough to support Cu wires firmly against chip pads and endure high bonding parameters were first evaluated by 3D finite element modeling (FEM) of the Cu heavy wire bonding process. The FEM results indicated that an electroless plated Ni layer may be used as the primary candidate for the pad metallization of Cu heavy wire bonding because it enables the reinforcement of standard Al pads in power devices and allows for metallurgical interaction with Cu wires. Further, the deposition of the Ni layer entailed a simple protocol. The three major bonding parameters including force, ultrasonic energy, and time were optimized to achieve successful wire bonding of 300-μm-thick Cu wires to pads strengthened with Ni layers in power devices. Microstructures and compositions of the bonded interface were analyzed by transmission electron microscopy, which provided insight into the bonding characteristics between the Cu wires and the Ni pads. Reliability tests of the bonding were also carried out by the thermal shock test and pressure cooker test.

Key words

Cu heavy wire, diode, IGBT (Insulated Gate Bipolar Transistors), power module, wirebonding

I. Introduction

A power module is the key building element in almost all power electronic systems used in renewable energy production and electric driven vehicles, which are two of the fastest growing markets. It contains a set of power semiconductor switches interconnected into a specific topology and enclosed in a single case. Ultrasonic Al heavy wire (100 to 500 μm in diameter) bonding is most commonly used for electrically interconnecting the power semiconductors. Since there is an increasing demand for improving the reliability of conventional Al interconnections, replacing Al wires with Cu wires has gained much interest. The typical failure mode observed in the Al heavy wire bonding is wire lift-off, which is the result of crack initiation and propagation within the wire matrix due to the cyclic mechanical stress attributed to the mismatch of the coefficients of thermal expansion (CTE) of the Al wire and Si chips during power or thermal cycling. The higher mechanical strength of the Cu wires can help prevent crack formation and growth. Cu also offers much higher electrical and thermal conductivities compared to Al, which permits higher current densities to be carried in the power modules. In addition, Cu wire bonding is also a more appropriate interconnection solution for next generation power modules that may be expected to widely adopt wide band gap power devices such as GaN and SiC, which will be operated at higher temperatures than typical Si-based devices.

When applying Cu heavy wire bonding to interconnections in power devices, one key requirement is to place the right metallization onto the chip pads. Cu heavy wires, which are at least twice as hard as Al heavy wires, require much higher bonding force and larger ultrasonic energy to achieve successful ultrasonic bonding. In power devices with standard Al metal pads (that are 3–10 μm in thickness and are made of pure Al or an Al alloy with Si or Si/Cu), the Cu heavy wires simply sink into the Al pads, leading to either very weak bonding with low bonding parameters or chip damage with high bonding parameters. The pad metallization for Cu heavy wire bonding is required to be sufficiently strong and thick to support the Cu wires firmly against the pad and to endure high bonding parameters. The metallization is also required to provide metallurgical bondability with Cu wires. Otherwise, bonding between the pads and wires will not be achieved. Previous studies have considered a thick Cu layer as pad metallization for Cu heavy wire bonding [1-3]. Schneider-Ramelow et al. [1] and Siepe et al. [2] reinforced their power device pads with electroplated Cu layers. In the Danfoss Buffer Bond (DBB) approach, Cu buffer layers were attached on top of diode pads with Ag sintering materials [3].

In this study, various chip pad metallizations including Cu layers as well as Ni layers have been considered for Cu heavy wire bonding. Different kinds of these metallizations with varying thicknesses were evaluated by 3D finite element modeling (FEM) of Cu heavy wire bonding interconnection. Ni layer obtained by electroless plating was chosen because reinforcement of the power device pads could be achieved with thinner layers in comparison to Cu layers. Further, the Ni layer allowed for metallurgical interaction with the Cu wires, could be deposited with ease without plating any seed layer, and did not require an additional bonding layer such as Ag sintering. In this work, we demonstrate a half-bridge power module in which four IGBTs and freewheeling diodes for each IGBT in both upper and lower arms are all interconnected with Cu heavy wires. The strength of the bonded Cu wires was evaluated by pull and shear testing. Microstructures and compositions at the bonded interface were analyzed by transmission electron microscopy (TEM). Reliability tests including the thermal shock and pressure cooker test (PCT) were also carried out.

II. 3D FEM of Cu Heavy Wire Bonding

The whole process of Cu heavy wire bonding was analyzed with 3D FEM, as shown in Fig. 1. The model consisted of a wedge tool, wire, and a power chip. Considering the typical layer structure of the power switch devices, the chip was simply modeled to consist of a sequential stack of 3-μm-thick Al pad, 1-μm-thick SiO_2 layer, and 200-μm-thick Si. Cu heavy wires with a thickness of 300 μm and a wedge with dimensions identical to that used in our experiments were also modeled. The Cu wires and the Al pad were assumed to be elastoplastic [4-6], while the Si chip, the oxide layer, and the wedge were assumed to be elastic. A commercial finite element code, ABAQUS, with an implicit solution was used.

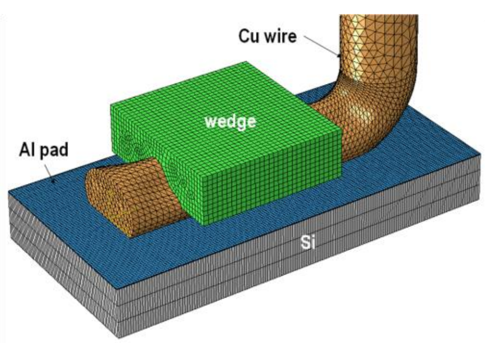

Fig. 1 The 3D FEM of Cu Heavy Wirebonding.

To model the ultrasonic wire bonding as close as possible to the actual bonding, it is critical to first understand the actual ultrasonic wire bonding process and bonding mechanism. The most plausible explanation for how ultrasonic wire bonding is fabricated is summarized below. It is to be noted that a clear explanation is yet to be proposed. Subsequent to bringing a wire down to the bond pad, wire bonding begins with applying a force to the wire through the wedge that will hold the wire firmly against the pad throughout the bonding process. Once the force applied reaches its set value, ultrasound is triggered. Here, the ultrasonic energy generated during wire bonding has two major contributions in the bond formation. First, the ultrasonic energy lowers the yield strength of the wire [7], resulting in a large deformation even with a small bond force, which in turn provides an intimate contact between the wire and the pad. Second, the ultrasonic energy also causes the wedge to cyclically and rapidly vibrate. The translational movement of the wedge can break the brittle oxide layers on the wire and the bond pad surfaces and sweep them aside to expose new metal surfaces [8]. The exposure of new surface areas can also be explained by the slip [9]. The cyclic wedge movement creates and moves dislocations at the interface between the wire and the bond pad, which allows atomic planes to slip over each other, generating new surfaces that are free of oxides and contamination. In any case, the newly exposed metal pad surfaces form an ultrasonic diffusion bond with the wire. Depending on the metals used for the wire and the bond pad, the phase that joins the wire to the bond pad may be an intermetallic compound (an ordered alloy) or a disordered alloy. The intermetallic compound typically forms only between metals that mix well over certain composition ranges, while the disordered phase forms when the metal from the wire and that from the pad dissolve in all portions [9].

Similar to the actual wire bonding process, our modeling began with applying a vertical force to the wire through the wedge. Here, the wire was initially assumed to contact onto the pad surface. A constant force of 6000 g was uniformly applied to the top surface of the wedge, which was equivalent to 150 MPa. Since, in our standard implicit modeling, it was difficult to capture the rapid and large wire plastic deformation that occurs by the ultrasonic softening, the wire was meshed to possess a deformed shape from the beginning (Fig. 1). The contact area of the wire with the bond pad surface was about 0.34 mm^2. Under the applied vertical force, the wedge moved back and forth along the wire under horizontal force control (-1300 g–1300 g), which yielded a horizontal displacement of 1–2 μm. Multiple ultrasonic vibrations are applied for 50–150 ms in the real heavy wire bonding process; however, here, a total of 5 cycles were repeated for simplicity.

Fig. 2 shows the contour plots of the von Mises stress for the Al pads, SiO_2 layer, and Si along with the equivalent plastic strain for the Al pads when Cu heavy wire bonding was made on standard Al pads of power devices.

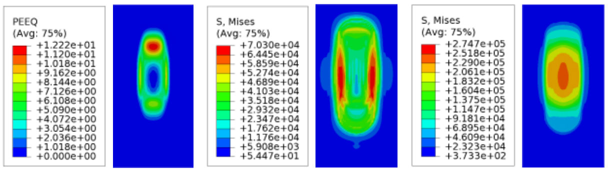

(a) (b) (c)

Fig. 2 Contour Plots of (a) the Equivalent Plastic Strain of Al pads and the von Mises Stress of (b) Al pads and (c) Si Chips.

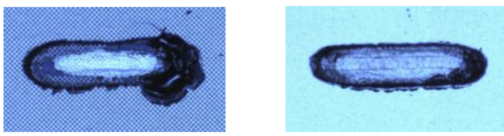

(a) (b)

Fig. 3 The Typical Chip Cratering observed during Cu Heavy Wirebonding on the Al Pads of (a) IGBT and (b) Diode.

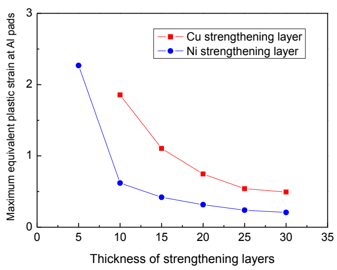

Fig. 4 The Equivalent Plastic Strain of Al Pads Reinforced with Ni and Cu Strengthening Layers.

The plastic deformation in the bottom surface of the Al pads facing the Si chips is to be carefully observed here since this plastic deformation is known to activate the slip system of Si, ultimately leading to chip breakage or cratering [10-11]. The Al pad deformation was concentrated on either the heel or the toe side at the periphery of the bonds and not at the central area. These severe plastic deformation sites were exactly consistent with the cratering sites observed during the actual Cu heavy wire bonding onto Al pads shown in Fig 3. Thus, it can be seen that in order to successfully achieve Cu heavy wire bonding in power devices without any chip failures, it is necessary to reduce or avoid the severe plastic deformation on the Al pads.

We considered introducing a strengthening layer of either Ni or Cu onto the Al pad because they are both harder than Al. Further, both Ni and Cu can be processed with simplicity in many different ways. The contribution of the strengthening layers to the Cu wire bonding was also evaluated through the FEM. The strengthening layers were added on top of the Al pads in the models of Fig. 1. Fig. 4 shows the plot of the largest plastic strain at the Al pads for various thicknesses of each strengthening layer. Irrespective of the kind of strengthening layers introduced, the plastic deformation of the Al pads was significantly reduced. However, the thicker strengthening layers, lower was the plastic deformation of the Al pads. Because of the higher hardness of the Ni layer than the Cu layer, plastic deformation of the Al pads was more reduced with the Ni layer during Cu heavy wire bonding. Thus, the Ni layer was primarily considered as the pad strengthening layer for our study.

III. Power Module with Cu Wire Bonding

A. Power Module

Fig. 5 shows the schematic of the cross section of the power module employed to evaluate Cu heavy wire bonding. Power devices of IGBTs and diodes were attached onto the direct bonded ceramic (DBC) substrate. The DBC substrate was composed of Al_2O_3, a ceramic insulator, onto which pure Cu metal layers were attached. For die bonding onto the DBC substrate, sintering with nanosized silver paste was used. This technique is emerging as an alternative lead-free die attachment solution in power modules because of the superior electrical, thermal, and mechanical properties it can provide when compared to conventional Sn-Ag-Cu soldering [1, 12]. All the DBC substrates used were finished with immersion silver, which was favorable for the sintering. The details of the sintering process have been described in our previous study [12].

B. Nickel Strengthening Layers on the Power Device Pads

Various Ni deposition techniques including vacuum deposition and wet chemical process are available for fabricating the nickel layers. The wet process is more preferable in terms of cost and mass production. There are two common wet processes that enable the deposition of a Ni layer onto the Al pads. These include electrolytic and electroless plating. Electrolytic plating of Ni requires a seed layer to provide an electrically conductive path, while the electroless Ni plating does not require such a seed layer and thus offers the advantage of process simplicity being based on a controlled chemical reduction reaction that is catalyzed by the metal or alloy being deposited. Electroless plating of Ni was chosen to fabricate the reinforcing layers on the Al pads on our IGBT and diode devices. The plating was carried out after attaching all the chips onto the DBC, which allows for better control of the warpage of the metalized chips. Further, simple plating masking was applied to the areas that required protection from unwanted plating. The entire plating process, which included conditioning, acid etching, zincation, and electroless plating, was carefully optimized to specifically ensure good adhesion of the plated Ni onto the Al pad layers.

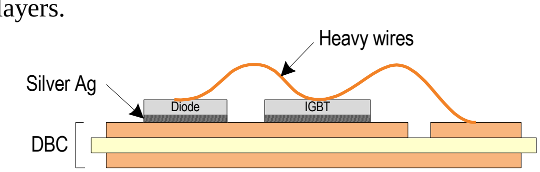

Fig. 5 The Schematic Cross-Section of Power Module to Evaluate Cu Heavy Wirebonding.

C. Copper Heavy Wire Bonding

The Cu heavy wire bonding was prepared with 300-μm-thick Cu (>99.99%) wires and Orthodyne heavy wire bonder (Irvine, CA) was used. The wire bonding quality is determined by three process parameters in the wire bonder i.e., the bonding force, ultrasonic power, and bonding time. While low bond force and insufficient ultrasonic power and time lead to weak or under-deformed bonds and chip cratering, high force and excessive ultrasonic power and time induce bond heel cracking, excessive wire deformation, and chip cratering/breakage. It is critical to find the optimum combination of these three parameters for successful Cu heavy wire bonding. The bonding window for Cu heavy wire bonding on the electroless Ni plated layer was identified by thorough optimization of the three parameters.

D. Characterization and Reliability of the Bonded Cu Heavy Wires

Pull and shear tests were carried out on the bonded wires using DAGE 4000 tester. The crystal structure of the electroless Ni deposit was investigated by X-ray diffraction (XRD), with a Phillips X'pert Pro diffractometer employing Cu Kα (1.54Å) radiation. TEM samples of the wires bonded onto the chip pads were prepared with Helios NanoLab 400S focused ion beam (FIB) equipment. Then, the bond interface was examined with Tecnai G2 F20S-TWIN TEM at the acceleration voltage of 200 kV. The compositional analysis of the bonded interface by energy dispersive X-ray spectrometry (EDS) was also carried out in the scanning TEM (STEM) modes with a probe diameter of 0.6 nm. All the TEM samples were cut parallel to the axial direction of the wire (i.e., the ultrasonic vibration direction). Further, thermal shock testing was performed between -40 and 150 ℃ with a dwell time of 30 min at each temperature. Standard PCT tests were carried out by exposing the fabricated power module to 121 ℃ and 2 atm pressure at 100% relative humidity for up to 168 h.

IV. Results and Discussion

Fig. 6 shows the cross section of the Ni layers obtained by electroless deposition on the Al pads of the IGBT device. The electroless process yielded uniform and conformal Ni layers on top of the Al pads. The EDS data (not shown here) revealed that the electroless Ni deposit contained 8.6 wt% of phosphorous.

Thorough optimization of the wire bonding parameters resulted in successful wire bonding of the 300-μm-thick Cu wires to the strengthened pads of the power devices, as shown in Fig. 7. All the electrical interconnections for the half-bridge power module were fabricated by Cu heavy wire bonding. Both the upper and lower arms in the half-bridge circuit consisted of four IGBTs and four diodes connected antiparallelly to the IGBTs. Failures such as pad-peeling or chip breakage were absent during wire bonding. Further, neither non-stick nor excessive wire deformation was observed. Simple electrical tests confirmed that the half-bridge power module functioned properly. The bonding parameters were thus assumed to be well optimized. The wire pull strength could reach over 1900 g on both the IGBT and diode chips, as listed in Table 1. All the shear strength values were above 2.7 kg. As a general quality index for heavy wire bonding, the bond pull strength is required to be equal to the wire breaking load, while the shear value should be >1.5 times the load [13]. Considering that the breaking load of the Cu wires that were used in this study ranges from 1600 to 1800 g, both the pull and shear strengths obtained were reasonable. During the pull tests, much of the failure occurred at the mid-span of wires, which once again confirmed the soundness of the bonding. Despite the reasonable shear strength value obtained, the shear test failure occurred at the interface between the Cu wires and the Ni pads without leaving much of the wire bond nugget on the pads.

Table 1 Pull and Shear Strength of the Bonded Cu Heavy Wires (The values in parentheses are standard deviation).

	IGBT	Diode
Pull Strength (gf)	1982 (90)	2157 (78)
Shear Strength at 1st bond (kgf)	2.78 (0.02)	3.02 (0.22)
Shear Strength at 2nd bond (kgf)	2.83 (0.13)	3.06 (0.03)

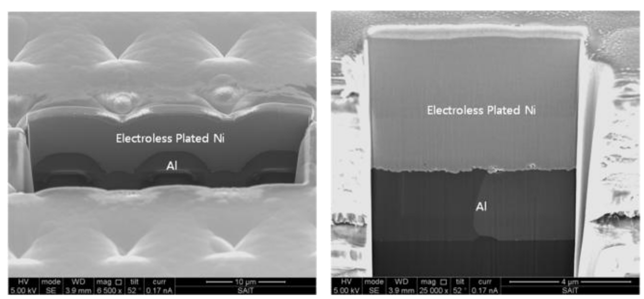

(a) (b)

Fig. 6 The Electroless Plated Ni Layers on the Al Pads of (a) IGBT and (b) Diode.

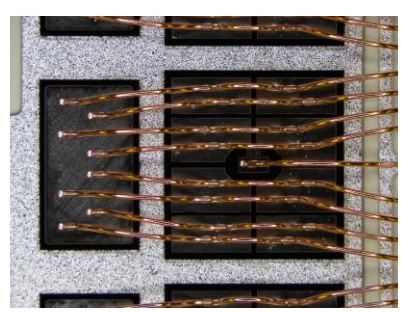

Fig. 7 The Diode and IGBT Chips Interconnected by 300-μm-thick Cu Wires in the Half-Bridge Power Module

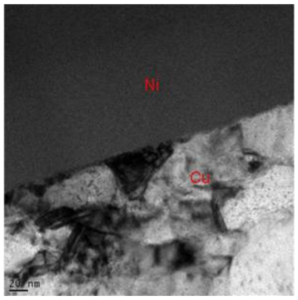

Fig. 8 The TEM Image of the Bond Interface between Cu wires and Electroless Plated Ni Layer.

Fig. 8 shows the typical TEM image of the interfacial morphologies at the Cu wire-Ni bond pads. The Cu wires were composed of polycrystalline structures, while crystalline structures were absent at the Ni pads generated by electroless plating. This was consistent with the results of the X-ray diffraction (XRD) analysis of the Ni layer obtained by Electroless plating (not shown here). The amorphous structure of the electroless Ni was confirmed from the single broad peak at $2\theta = 45°$. Similar to the microstructure observed at the bonding interface between Al heavy wire and Al pads of power semiconductors [14], the Cu wires seemed to experience severe plastic deformation and dynamic recrystallization during wire bonding, which resulted in extremely fine grain sizes of less than 0.2 μm. More importantly, surface oxides of either Ni or Cu were absent at the interface. Further, contaminants were also absent, which can lead to strong metallurgical bonding between the Cu wires and the Ni bond pads.

The results of the STEM-EDS analysis clearly showed the metal diffusion of Cu and Ni atoms at the bonding interface (Fig. 9). Both Ni and P were found to diffuse into the Cu wire side, while Cu was not detected in the Ni pad layers obtained by electroless plating. Many diffusion studies on Ni and Cu polycrystalline material couples showed the ability of Ni atoms to diffuse into the Cu crystal through the various available diffusion paths such as grain boundaries, lattice defects, and lattice when the Ni/Cu couples were thermally activated [15]. Similar to the thermal diffusion process, ultrasonic energy could have activated the diffusion of both Ni and P atoms in the Ni-P layers obtained by electroless plating to move into Cu wire side during wire bonding.

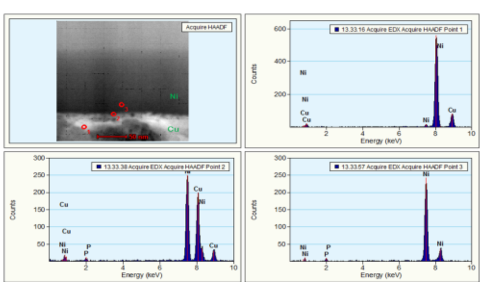

Fig. 9 The STEM-EDS Analysis of the Bond Interface between Cu Wires and Electroless Plated Ni Layer.

However, the Ni-P layer obtained by electroless plating is known to be a very effective barrier layer against Cu diffusion, even though polycrystalline Ni allows the diffusion of Cu atoms [16-17]. The as-plated Ni-P layer obtained by electroless deposition with its amorphous structure is a more effective barrier layer than the crystalline Ni-P layer obtained by annealing the as-plated Ni-P layer above 300 ℃ [14]. This is because the amorphous structure can better eliminate rapid paths for Cu diffusion such as grain boundaries and dislocation defects. This explains the reason for the absence of Cu atoms in the Ni-P layers obtained by electroless plating. Hence, the ultrasonic diffusion of Ni and P atoms from the Ni pad layers into Cu wires can be ascribed to the bonding of Cu heavy wires on the electroless Ni-P pads and the bonding strength may be expected to be primarily dependent on the diffusivity of both Ni and P atoms into the Cu wire side during ultrasonic wire bonding.

The reliability of the bonded Cu heavy wires was evaluated by thermal shock testing. Fig. 10 shows the change in the pull and shear strengths of the Cu heavy wire bonding reported here with increasing number of thermal shock cycles. Significant drop in either of the strength values was absent. The strength values of most of the bonds rather increased with number of thermal shock cycles. This is thought to be certainly related to the thermal diffusion of the Ni and P atoms from the Ni pads to the Cu wires.

Both Cu wires and Ni pads are highly susceptible to oxidation and more seriously in a humid environment. Several studies have also claimed that the shear strength of Cu ball wire bonding made on Al pads could significantly drop because of corrosion at the bonding interface [18]. The corrosion resistance of the bonding between Cu heavy wires and Ni pads reported here needs to be investigated. Fig. 11 compares the shear and pull strength values for the Cu heavy wire bonding reported in this paper before and after PCT, which is the most common accelerated test used to measure the resistance to moisture penetration and the resultant effects of galvanic corrosion. Any significant changes in either pull or shear strength measured were absent, which indicated that the bonding of Cu heavy wires on the Ni pad was immune to corrosion.

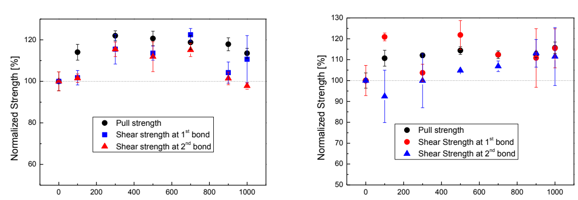

(a) (b)

Fig. 10 The Change in Pull/Shear Strength during Thermal Shock Testing for (a) IGBT and (b) Diode.

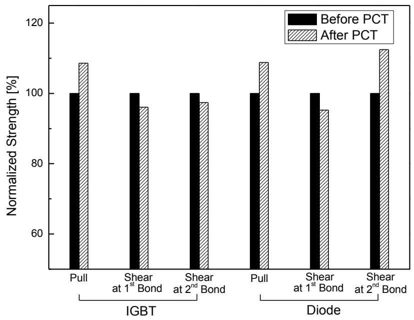

Fig. 11 The Pull/Shear Strength before and after PCT.

V. Conclusion

Cu heavy wire bonding was successfully applied to four IGBTs and freewheeling diodes for each IGBT in both upper and lower arms of a half-bridge power module that were electrically interconnected. 3D FEM of the Cu heavy wire bonding process was performed on various chip pad metallizations including the standard Al pads used in power devices. The FEM results showed that the Cu wire bonding on the standard Al pads induced severe plastic deformation on either the heel or the toe side at the periphery of the bonds, which was later confirmed to be consistent with the cratering sites observed during the actual Cu heavy wire bonding onto the Al pads. The modeling also indicated that the plastic deformation could be most significantly reduced by introducing Ni layers on top of the Al pads. The Al pads of commercially available IGBT and diode chips were thus reinforced by electroless Ni plating. Wire bonding with 300-μm-thick Cu wires was successfully carried out on the Ni pads without bonding failure such as cratering, non-stick, and pad peeling. The bonding of Cu wires on the Ni pads yielded reasonable values of pull and shear strengths. The TEM analysis of the bonding interface revealed that the ultrasonic diffusion of Ni and P atoms from the Ni pads deposited by electroless plating into the Cu wires could be ascribed to their solid bonding. Surface oxides of neither Ni nor Cu were present at the interface and contaminants were found to be absent. The temperature shock test and PCT induced no significant changes in the pull and shear strengths.

Acknowledgment

Authors are deeply grateful to Mr. Euijin Lee, Mr. Wonho Choi, and Mr. Sukgu Koh from Atotech Korea Ltd. and Atotech Deutschland GmbH for their valuable technical support toward the electroless Ni plating employed in this study.

References

[1] M. Schneider-Ramelow, M. Hutter, H. Oppermann, J-M. Gohre, S. Schmitz, E. Hoene and K-D. Lang, "Technologies and trends to improve power electronic packaging," in *Proc. 44th Intenational Sysmposium on Microelectronics*," Long Beach, CA, 2011, pp. 430-437.

[2] D. Siepe, R. Bayerer and R. Roth, "The future of wire bonding is? Wire bonding!," in *Proc. 6th International Conference on Integrated Power Electronics Systems*, Nuremberg, 2010, paper 3.7.

[3] S. Haumann, J. Rudzki, F. Osterwald, M. Becker and R. Eisele, "Novel bonding and joining technology for power electronics," in *Proc. 28th Annual IEEE Applied Power Electronics Conference and Exposition*, Long Beach, CA, 2013, pp. 622-626.

[4] P. Agostinetti, M. Dalla Palma, S. Dal Bello, B. Heinemann, R. Nocentini, C. Zauner, H. Langer and J. Klammer, "Investigation of the thermo-mechanical properties of electro-deposited copper for ITER," *Journal of Nuclear Materials*, vol 417, Oct. 2011, pp.924-927.

[5] D.-J. Kim, M.J. Kim, J.S. Kim and H.P. Kim, "Material characteristics of Ni–P–B electrodeposits obtained from a sulfamate solution," *Surface & Coatings Technology*, vol. 202, Mar. 2008, pp. 2519-2526.

[6] N. Kamikawa, X. Huang, N. Tsuji, N. Hansen, "Strengthening mechanisms in nanostructured high-purity aluminium deformed to high strain and annealed," *Acta Materialia*, vol. 57, Aug. 2009, pp. 4198-4208

[7] B. Langenecker, "Effects of ultrasound on deformation characteristics of metals," *IEEE Transaction on Sonics and Ultrasonics*, vol. SU-13, Mar. 1966, pp. 1-8.

[8] L. Levine, "The ultrasonic wedge bonding mechanism: Two theories converge," in *Proc. The International Symposium on Microelectronics, ISHM*, Long Beach, CA, 1995, pp. 242-246.

[9] C.D. Breach and F.W. Wulff, "A brief review of selected aspects of the materials science of ball bonding," *Microelectronics Reliability*, vol. 50, Jan. 2010, pp. 1-20.

[10] V.H. Winchell and H. Berg, "Enhancing ultrasonic bond development", *IEEE Transactions on Components, Hybrids and Manufacturing Technology*, vol. CHMT-1, Sept. 1978, pp. 211-219.

[11] V.H. Winchell, "An evaluation of silicon damage resulting from ultrasonic wire bonding," in *Proc. 14th Annual Reliability Physics Symposium*, Las Vegas, NE, 1976, pp. 98-107.

[12] Y. Byun, C. Jeong, J.-W. Yoon, C.-H. Kim, C.-S. Kim, B.-W. Lee, S.W. Booh and U-I. Chung, "A novel and simple fabrication technology for high power module with enhanced thermal performance," in *Proc. 2012 IEEE Vehicle Power and Propulsion Conference (VPPC)*, Seoul, Korea, 2012, pp. 1070-1073.

[13] J. Ling, T. Xu, C. Luechinger, P. Backus and O. Worm, "Large-Cu-wire wedge bonding on wafers with Cu pad metallization," in *Proc. International Exhibition and Conference for Power Electronics, Intelligent Motion, Renewable Energy and Energy Management*, Nuremberg, 2012, paper-103.

[14] J. Goehre, M. Schneider-Ramelow, U. Geiβler and K.-D. Lang, "Interface degradation of Al heavy wire bonds on power semiconductors during active power cycling measured by the shear test," in *Proc. 6th International Conference on Integrated Power Electronics Systems*, Nuremberg, 2010, paper 3.4.

[15] O. Arnould and F. Hild, "Long-term life of Ni/Cu bellows: effect of diffusion on thermomechanical properties," *Defect and Diffusion Forum*, vol. 203-205, 2002, pp. 61-80.

[16] E.J. O'Sullivan, A.G. Schrott, M. Paunovic, C.J. Sambucetti, J.R. Marino, P.J. Bailey, S. Kaja and K.W. Semkow, "Electrolessly deposited diffusion barriers for microelectronics," *IBM Journal of Research and Development*, vol. 42, Sep. 1998, pp. 607-620.

[17] J.F. Rohan and G. O'Riordan, "Characterization of the electroless nickel deposit as a barrier layer/under bump metallurgy on IC metallization," *Microelectronic Engineering*, vol. 65, Jan. 2003, pp. 77-85.

[18] T. Uno, "Bond reliability under humid environment for coated copper wire and bare copper wire," *Microelectronics Reliability*, vol. 51, Jan. 2011, pp. 148-156.